Pump RIN-induced impairments in unrepeatered transmission systems using distributed Raman amplifier

Jingchi Cheng,[1,2] Ming Tang, [1,*] Alan Pak Tao Lau, [2] Chao Lu, [3] Liang Wang, [3] Zhenhua Dong, [2] Syed Muhammad Bilal, [4] Songnian Fu, [1] Perry Ping Shum, [5] and Deming Liu [1]

[1]*National Engineering Laboratory for Next Generation Internet Access System, School of Optics and Electronic Information, Huazhong University of Science and Technology, Wuhan, 430074, China*

[2]*Photonics Research Centre, Department of Electrical Engineering, The Hong Kong Polytechnic University, Hong Kong*

[3]*Photonics Research Centre, Department of Electronic and Information Engineering, The Hong Kong Polytechnic University, Hong Kong*

[4]*Politecnico di Torino, DET, Corso Duca Degli Abruzzi 24, Torino, Italy*

[5]*Photonics Centre of Excellence, School of Electrical and Electronic Engineering, Nanyang Technological University, 637553 Singapore*

[*]*tangming@mail.hust.edu.cn*

Abstract: High spectral efficiency modulation format based unrepeatered transmission systems using distributed Raman amplifier (DRA) have attracted much attention recently. To enhance the reach and optimize system performance, careful design of DRA is required based on the analysis of various types of impairments and their balance. In this paper, we study various pump RIN induced distortions on high spectral efficiency modulation formats. The vector theory of both 1st and higher-order stimulated Raman scattering (SRS) effect using Jones-matrix formalism is presented. The pump RIN will induce three types of distortion on high spectral efficiency signals: intensity noise stemming from SRS, phase noise stemming from cross phase modulation (XPM), and polarization crosstalk stemming from cross polarization modulation (XPolM). An analytical model for the statistical property of relative phase noise (RPN) in higher order DRA without dealing with complex vector theory is derived. The impact of pump RIN induced impairments are analyzed in polarization-multiplexed (PM)-QPSK and PM-16QAM-based unrepeatered systems simulations using 1st, 2nd and 3rd-order forward pumped Raman amplifier. It is shown that at realistic RIN levels, negligible impairments will be induced to PM-QPSK signals in 1st and 2nd order DRA, while non-negligible impairments will occur in 3rd order case. PM-16QAM signals suffer more penalties compared to PM-QPSK with the same on-off gain where both 2nd and 3rd order DRA will cause non-negligible performance degradations. We also investigate the performance of digital signal processing (DSP) algorithms to mitigate such impairments.

OCIS codes: (060.1660) Coherent communications; (230.4480) Optical amplifiers.

References and links

1. X. Zhou, L. E. Nelson, R. Isaac, P. Magill, B. Zhu, D. W. Peckham, P. Borel, and K. Carlson, "1200km Transmission of 50GHz spaced, 5×504-Gb/s PDM-32-64 hybrid QAM using Electrical and Optical Spectral Shaping," in Tech. Digest of the Conference on Optical Fiber Communication (2012), paper OM2A.2.
2. X. Zhou, L. E. Nelson, R. Isaac, P. D. Magill, B. Zhu, P. Borel, K. Carlson, and D. W. Peckham, "12000km Transmission of 100GHz spaced, 8×495-Gb/s PDM Time-Domain Hybrid QPSK-8QAM Signals," in Tech. Digest of the Conference on Optical Fiber Communication (2013), paper OTu2B.4.

#234455 - $15.00 USD Received 11 Feb 2015; revised 16 Apr 2015; accepted 19 Apr 2015; published 27 Apr 2015

3. L. E. Nelson, X. Zhou, B. Zhu, M. F. Yan, P. W. Wisk, and P. D. Magill, "All-Raman-amplified, 73 nm seamless band transmission of 9 Tb/s over 6000 km of fiber," IEEE Photonics Technol. Lett. **26**(3), 242–245 (2014).
4. R.-J. Essiambre, P. Winzer, J. Bromage, and C. H. Kim, "Design of bidirectionally pumped fiber amplifiers generating double Rayleigh backscattering," IEEE Photonics Technol. Lett. **14**(7), 914–916 (2002).
5. C. R. S. Fludger, V. Handerek, and R. J. Mears, "Pump to signal RIN transfer in Raman fiber amplifiers," J. Lightwave Technol. **19**(8), 1140–1148 (2001).
6. Q. Lin and G. P. Agrawal, "Vector theory of stimulated Raman scattering and its application to fiber-based Raman amplifiers," J. Opt. Soc. Am. B **20**(8), 1616–1631 (2003).
7. S. Sergeyev, S. Popov, and A. T. Friberg, "Modeling polarization-dependent gain in fiber Raman amplifiers with randomly varying birefringence," Opt. Commun. **262**(1), 114–119 (2006).
8. E. S. Son, J. H. Lee, and Y. C. Chung, "Statistics of polarization-dependent gain in fiber Raman amplifiers," J. Lightwave Technol. **23**(3), 1219–1226 (2005).
9. J. Bromage, "Raman amplification for fiber communication systems," J. Lightwave Technol. **22**(1), 79–93 (2004).
10. M. D. Mermelstein, K. Brar, and C. Headley, "RIN transfer measurement and moldeling in dual-order Raman fiber amplifiers," J. Lightwave Technol. **21**(6), 1518–1523 (2003).
11. S. Jiang and P. Gallion, "Theoretical analysis on the PMD-assisted pump-to-signal noise transfer in distributed fiber Raman amplifiers," J. Lightwave Technol. **25**(10), 3185–3192 (2007).
12. J. Cheng, M. Tang, S. Fu, P. P. Shum, and D. Liu, "Relative phase noise induced impairment in M-ary phase-shift-keying coherent optical communication system using distributed fiber Raman amplifier," Opt. Lett. **38**(7), 1055–1057 (2013).
13. J. Cheng, M. Tang, S. Fu, P. P. Shum, D. Liu, M. Xiang, Z. Feng, and D. Yu, "Relative phase noise estimation and mitigation in Raman amplified coherent optical communication system," Opt. Express **22**(2), 1257–1266 (2014).
14. J. Cheng, M. Tang, S. Fu, P. P. Shum, D. Yu, L. Wang, and D. Liu, "Relative phase noise-induced phase error and system impairment in pump depletion/nondepletion regime," J. Lightwave Technol. **32**(12), 2277–2286 (2014).
15. J. Wu, J. Cheng, M. Tang, L. Deng, F. Songnian, P. P. Shum, and D. Liu, "Relative phase noise induced impairment in CO-OFDM optical communication system with distributed fiber Raman amplifier," Opt. Lett. **39**(10), 2841–2844 (2014).
16. T. J. Xia, D. L. Peterson, G. A. Wellbrock, D. Chang, P. Perrier, H. Fevrier, S. Ten, C. Tower, and G. Mills, "557-km Unrepeatered 100G Transmission with Commercial Raman DWDM System, Enhanced ROPA, and Cabled Large Aeff Ultra-Low Loss Fiber in OSP Environment," in Tech. Digest of the Conference on Optical Fiber Communication (2014), paper Th5A.7.
17. B. Zhu, P. Borel, K. Carlson, X. Jiang, D. W. Peckham, and R. J. Lingle, "Unrepeatered transmission of 3.2-Tb/s (32×120-Gb/s) over 445-km fiber link," IEEE Photon. Technol. Lett. **25**(19), 1863–1866 (2013).
18. H. Bissessur, P. Bousselet, D. A. Mongardien, and I. Brylski, "Ultra-long 10 Gb/s Unrepeatered WDM Transmission up to 601 km," in Tech. Digest of the Conference on Optical Fiber Communication (2010), paper OTuD.6.
19. M. Winter, C.-A. Bunge, D. Setti, and K. Petermann, "A statistical treatment of cross-polarization modulation in DWDM systems," J. Lightwave Technol. **27**(17), 3739–3751 (2009).
20. G. P. Agrawal, Nonlinear Fiber Optics, 3rd ed. (Academic, 2000).
21. Q. Lin and G. P. Agrawal, "Effects of polarization-mode dispersion on cross-phase modulation in dispersion-managed wavelength-division-multiplexed systems," J. Lightwave Technol. **22**(4), 977–987 (2004).
22. D. Chang, H. D. Pedro, P. Perrier, H. Fevrier, S. Ten, C. Towery, I. Davis, and S. Makovejs, "150 x 120 Gb/s Unrepeatered Transmission over 333.6 km and 389.6 km (with ROPA) G.652 Fiber," in Proc. European Conference on Optical Communications (2014), paper Tu.1.5.4.
23. H. Bissessur, C. Bastide, S. Dubost, S. Etinne, and D. Mongardien, "8 Tb/s unrepeatered transmission of real-time processed 200 Gb/s PDM 16-QAM over 363 km," in Proc. European Conference on Optical Communications (2014), paper Tu.1.5.3.
24. J. D. Downie, J. Hurley, I. Roudas, D. Pikula, and J. A. Garza-Alanis, "Unrepeatered 256 Gb/s PM-16QAM transmission over up to 304 km with simple system configurations," Opt. Express **22**(9), 10256–10261 (2014).
25. A. Bononi, P. Serena, N. Rossi, and D. Sperti, "Which is the Dominant Nonlinearity in Long-haul PDM-QPSKCoherent Transmissions," in Proc. European Conference on Optical Communications (2010), paper Th.10.E.1.
26. L. Li, Z. Tao, L. Liu, W. Yan, S. Oda, T. Hoshida, and J. C. Rasmussen, "Nonlinear Polarization Crosstalk Canceller for Dual-Polarization Digital Coherent Receivers," in Tech. Digest of the Conference on Optical Fiber Communication (2010), paper OWE3.

1. Introduction

Distributed Raman amplifier (DRA) is an enabling technology for contemporary coherent optical communication systems thanks to its large amplification bandwidth and low noise feature [1–3]. It is well known that with the appropriate gain allocation, bidirectional pumped

#234455 - $15.00 USD Received 11 Feb 2015; revised 16 Apr 2015; accepted 19 Apr 2015; published 27 Apr 2015

DRA can achieve optimal performance. The design of gain map depends on the balance of various types of distortions caused by forward and backward pumping. For example, higher gain from forward pumps will enhance the relative intensity noise (RIN) transfer effect as well as signal's nonlinearity, and higher gain from backward pumps will introduce signal-to-noise ratio (SNR) tilting problem. The double Rayleigh backscattering (DRB) noise should also be considered in such analysis [4]. The research of DRA has been extensively performed in traditional intensity-modulation direct-detection (IM/DD) systems [4–11]. However, extending such analysis to coherent optical communication systems may not be intuitive, since the phase of multi-level modulation formatted signals was usually not considered. Recently, we have shown through theory and simulation that, in the case of 1st order DRA, the Raman pump's intensity noise will cause not only intensity distortions of signals, but also phase deterioration [12–15]. Such phase noise, originating from cross-phase modulation (XPM) effect, is defined as relative phase noise (RPN). It is demonstrated that RPN generated from forward pumps is much more harmful than that from backward pumps, because the huge walk-off between signals and backward pumps can effectively average out the noise. Monte Carlo simulations suggested that for forward pumped DRA based long-haul transmission over 1000 km, the differential-coded QPSK signals can tolerate up to −120 dB/Hz pump RIN without suffering notable impairments [13].

In addition to multi-span based long-haul systems, DRA is also indispensable in unrepeatered transmissions, where point-to-point communication over hundreds of kilometers is achieved without in-line repeaters. Such architecture finds useful applications in the communication between islands or hostile areas. Longer reach can be obtained by using DRA, since it provides gain in the fiber itself and helps to improve the noise figure (NF). For example, T. J. Xia et al has achieved 557 km unrepeatered transmission of 100 Gb/s PM-QPSK signal with the use of 1st order DRA [16]. To further enhance the reach, higher-order DRA can be deployed, where the gain is penetrated deeper into the remote section of the fiber. A number of experimental studies using this technique have been reported. For example, B. Zhu et al has demonstrated 445 km transmission of 3.2 Tb/s WDM signals with PDM-QPSK modulation format using 2nd order DRA [17], and H. Bissessur et al has achieved 601 km unrepeatered transmission of 10 Gb/s RZ-DPSK signal based on 3rd order DRA [18]. The wide use of higher order DRA raises the question of how to study the interaction between higher order pumps and multi-level modulated signals. Since our previous investigation is confined to 1st order DRA, it is necessary to extend our model to higher order DRA case.

Another confinement of the previous study is that the polarization evolution is not addressed. Since polarization multiplexing is now a standard technique for multi-level modulation, it is necessary to take it into account.

Driven by these two motivations, we present a comprehensive study on the pump RIN induced impairments in the context of unrepeatered transmission systems in this paper. We first present Jones-matrix formalized vector theory of 1st and higher-order DRA, where polarization is taken into consideration. The pump RIN induced noise mechanisms on signal's amplitude, phase and polarization are pointed out and analyzed. The polarization deterioration is defined as relative polarization noise (RPolN), so as to keep the consistency with the previously defined terminologies. The impact of the distortions is first analyzed in a PM-QPSK based unrepeatered transmission via simulations. Results of 1st, 2nd and 3rd order DRA are compared. It is shown that only 3rd order DRA will induce non-negligible penalty with realistic pump RIN level. Next, the influence on PM-16QAM is studied at the same system configuration. More penalties are observed as expected. In the end, we investigate the performance of digital signal processing (DSP) algorithms in mitigating the phase and polarization degradation.

#234455 - $15.00 USD Received 11 Feb 2015; revised 16 Apr 2015; accepted 19 Apr 2015; published 27 Apr 2015

2. Theoretical modeling

2.1 Remarks on notations

In general, we adopt the notation presented in [19]. To distinguish two-dimensional complex vectors which describe the optical field in Jones space from their three-dimensional brethren in Stokes space, in this paper, we will use Dirac's bra-ket formalism, e.g., $\left|a\right\rangle = \left(a_x, a_y\right)^{\mathrm{T}}$, to denote Jones vectors. They are normalized such that $\left\langle A_p \middle| A_p \right\rangle$ equals the optical power, where $\left\langle A_p \right| = \left(a_x^*, a_y^*\right)$ is the conjugate transpose. Stokes vectors are denoted by bold letters, e.g., $\mathbf{S} = \left(S_1, S_2, S_3\right)^{\mathrm{T}}$, and unit vectors in Stokes space, describing a state of polarization (SOP), are decorated with a hat, as in $\hat{\mathbf{S}}$. Complex operators or matrices are decorated with a macron, such as $\overline{\mathbf{T}}$. For Pauli matrices:

$$\sigma_1 = \begin{pmatrix} 1 & 0 \\ 0 & -1 \end{pmatrix} \sigma_2 = \begin{pmatrix} 0 & 1 \\ 1 & 0 \end{pmatrix} \sigma_3 = \begin{pmatrix} 0 & -i \\ i & 0 \end{pmatrix} \tag{1}$$

and the Pauli vector $\boldsymbol{\sigma} = \left(\sigma_1, \sigma_2, \sigma_3\right)^{\mathrm{T}}$.

Some of the symbols used in the paper are listed below:

- A : electric field. Subscript x and y denote x and y polarizations, and p and s denote pump and signal respectively.
- P : power of light.
- β : propagation constant. Subscript 1 denotes inverse group velocity, and 2 denotes chromatic dispersion.
- $\delta\beta$: walk-off parameter.
- α : fiber attenuation.
- $\mathbf{B}$: residual fiber birefringence.
- γ : fiber nonlinearity coefficient.
- g_R : effective Raman gain efficient.
- D_p : PMD parameter.
- c : speed of light.
- A_{eff} : fiber effective mode area.

2.2 Vector theory of 1st order SRS

In [6], Jones-matrix formalized vector theory of 1st order SRS was proposed for the first time. The coupled nonlinear Schrodinger equations describing forward pumped DRA are:

#234455 - $15.00 USD Received 11 Feb 2015; revised 16 Apr 2015; accepted 19 Apr 2015; published 27 Apr 2015

$$\frac{d|A_p\rangle}{dz} = -\frac{\alpha_p}{2}|A_p\rangle - \frac{i}{2}\mathbf{B_p}\cdot\boldsymbol{\sigma}|A_p\rangle + \frac{i\gamma_p}{3}\left[2\langle A_p|A_p\rangle + \frac{\kappa_a}{\kappa_b}|A_p^*\rangle\langle A_p^*|\right]|A_p\rangle$$
$$+\frac{2i\gamma_p}{3}\left[(1+\delta_a)\langle A_s|A_s\rangle + (1+\delta_b)|A_s\rangle\langle A_s| + \left(\frac{\kappa_a}{\kappa_b}+\delta_b\right)|A_s^*\rangle\langle A_s^*|\right]|A_p\rangle \quad (2)$$
$$-\frac{1}{2}\left[g_2\langle A_s|A_s\rangle + g_1|A_s\rangle\langle A_s| + g_2|A_s^*\rangle\langle A_s^*|\right]|A_p\rangle$$

$$\frac{d|A_s\rangle}{dz} = -\frac{\alpha_s}{2}|A_s\rangle - \frac{i}{2}\mathbf{B}_s\cdot\boldsymbol{\sigma}|A_s\rangle + \frac{i\gamma_s}{3}\left[2\langle A_s|A_s\rangle + \frac{\kappa_a}{\kappa_b}|A_s^*\rangle\langle A_s^*|\right]|A_s\rangle$$
$$+\frac{2i\gamma_p}{3}\left[(1+\delta_a)\langle A_p|A_p\rangle + (1+\delta_b)|A_p\rangle\langle A_p| + \left(\frac{\kappa_a}{\kappa_b}+\delta_b\right)|A_p^*\rangle\langle A_p^*|\right]|A_s\rangle \quad (3)$$
$$+\frac{1}{2}\left[g_2\langle A_p|A_p\rangle + g_1|A_p\rangle\langle A_p| + g_2|A_p^*\rangle\langle A_p^*|\right]|A_s\rangle$$

where continuous wave (CW) is assumed for both pump and signal and ω_p/ω_s approximates 1. The parameters κ_a and κ_b are related to the Kerr and Raman response and usually $\kappa_a \approx \kappa_b$ [6]. The two dimensionless parameters δ_a and δ_b are related to the refractive index changes caused by Raman response and can be assumed that $\delta_a \approx 0$ and $\delta_b \approx 0$ since they are small compared to SPM and XPM contribution [20]. The Raman-gain parameters g_1 and g_2 account for the contributions from the isotropic and anisotropic nuclear response respectively, and in general, g_1 is much smaller than g_2 for optical fibers. Therefore, we can assume that $g_1 \approx 2g_R$ and $g_2 \approx 0$.

Most of the research work of SRS in IM/DD systems chose to transform the coupled equations in Stokes space [6–8], because they have simpler forms. The significant flaw of Stokes-matrix equations is that the phase information is not contained. Therefore, in order to cover all three dimensions including amplitude, phase and polarization, Jones-matrix formalized equations are a must. We focus on forward pumping only, because the backward pumps usually induce negligible impairments due to the huge walk-off.

Equations (2) and (3) can be modified if we consider the different group velocity between pump and signal, signal's dispersion (up to second order in this paper), and ignore the nonlinear effect from signal to pump and the SPM of signal. The modified equations can be rewritten as:

$$\frac{\partial|A_p\rangle}{\partial z} = -\frac{\alpha_p}{2}|A_p\rangle - \frac{i}{2}\mathbf{B_p}\cdot\boldsymbol{\sigma}|A_p\rangle - \beta_{1p}\frac{\partial|A_p\rangle}{\partial t} + \frac{i\gamma_p}{3}\left[2\langle A_p|A_p\rangle + |A_p^*\rangle\langle A_p^*|\right]|A_p\rangle \quad (4)$$

$$\frac{\partial|A_s\rangle}{\partial z} = -\frac{\alpha_s}{2}|A_s\rangle - \frac{i}{2}\mathbf{B}_s\cdot\boldsymbol{\sigma}|A_s\rangle - \beta_{1s}\frac{\partial|A_s\rangle}{\partial t} - \frac{i\beta_{2s}}{2}\frac{\partial^2|A_s\rangle}{\partial t^2}$$
$$+\frac{i2\gamma_s}{3}\left[\langle A_p|A_p\rangle + |A_p\rangle\langle A_p| + |A_p^*\rangle\langle A_p^*|\right]|A_s\rangle + g_R|A_p\rangle\langle A_p||A_s\rangle \quad (5)$$

The equations can be further simplified if we average over rapid polarization variations by adopting a rotating frame through a unitary transformation $|A_p\rangle = \bar{\mathbf{T}}|A_p'\rangle$, where the

#234455 - $15.00 USD Received 11 Feb 2015; revised 16 Apr 2015; accepted 19 Apr 2015; published 27 Apr 2015

transmission matrix satisfies $\frac{d\overline{\mathbf{T}}}{dz}=-\frac{i}{2}\mathbf{B_P}\cdot\boldsymbol{\sigma}\overline{\mathbf{T}}$. The averaging process is the same as that done in [20]. The final coupled equations are:

$$\frac{\partial\left|A_p\right\rangle}{\partial z}=-\delta\beta_1\frac{\partial\left|A_p\right\rangle}{\partial\tau}-\frac{\alpha_p}{2}\left|A_p\right\rangle+\frac{i8\gamma_p}{9}P_p\left|A_p\right\rangle \tag{6}$$

$$\begin{aligned}\frac{\partial\left|A_s\right\rangle}{\partial z}=&-\frac{\alpha_s}{2}\left|A_s\right\rangle-\frac{i\beta_{2s}}{2}\frac{\partial^2\left|A_s\right\rangle}{\partial\tau^2}-\frac{i}{2}\Omega\mathbf{b}\cdot\boldsymbol{\sigma}\left|A_s\right\rangle\\&+\left(\frac{i4\gamma_s}{3}+\frac{1}{2}g_R\right)P_p\left|A_s\right\rangle+\left(\frac{i4\gamma_s}{9}+\frac{1}{2}g_R\right)P_p\hat{\mathbf{P}}_\mathbf{p}\cdot\boldsymbol{\sigma}\left|A_s\right\rangle\end{aligned} \tag{7}$$

where we have introduced the common retarded reference frame with $\tau=t-\beta_{1s}z$ and drop the primes for notational simplification. The walk-off parameter $\delta\beta_1=\beta_{1p}-\beta_{1s}$, and the angular frequency shift $\Omega=\omega_p-\omega_s$. The relative local birefringence vector $\mathbf{b}$ shown in Eq. (7) is a zero-mean stochastic process in the asymptotically stationary regime (ASR), and its autocorrelation function (ACF) is [11]:

$$\left\langle\mathbf{b}(z_1)\mathbf{b}(z_2)\right\rangle=\frac{\overline{\mathbf{I}}}{3}D_p^2\frac{\exp\left(-\left|z_1-z_2\right|/L_C\right)}{2L_C} \tag{8}$$

with $\overline{\mathbf{I}}$ being the second-order unit tensor and L_C being the fiber correlation length.

Equations (6) and (7) describe the full field of Raman pump and signal. Each term corresponds to explicit physical meaning. The equation describing the pump is simple. Only walk-off, attenuation and SPM are considered, corresponding to the terms represented on the right side of Eq. (6). The equation describing the signal is more complex. The terms in the first row on right-hand side of Eq. (7) represent linear process, including attenuation, chromatic dispersion, and residual birefringence. The terms in the second row represent nonlinear process. The term $\frac{i4\gamma_s}{3}P_p\left|A_s\right\rangle$ represents averaged XPM and $\frac{1}{2}g_RP_p\left|A_s\right\rangle$ is the averaged Raman gain. These two effects rely only on the power of pump. The term $\frac{i4\gamma_s}{9}P_p\hat{\mathbf{P}}_\mathbf{P}\cdot\boldsymbol{\sigma}\left|A_s\right\rangle$ is referred to as XPolM and $\frac{1}{2}g_RP_p\hat{\mathbf{P}}_\mathbf{P}\cdot\boldsymbol{\sigma}\left|A_s\right\rangle$ is the polarization dependent Raman gain. These effects are polarization dependent.

2.3 Vector theory of higher-order SRS

The vector theory shown above can be extended to higher order SRS process. Take 2nd order SRS as an example. In 2nd order DRA, the power is transferred from 2nd order pump to signal via 1st order pump. Therefore, three equations are needed in this case. Following the same procedure and after some algebra, the final coupled equations are given as:

$$\begin{aligned}\frac{\partial\left|A_{p2}\right\rangle}{\partial z}=&-\delta\beta_1^{p2,s}\frac{\partial\left|A_{p2}\right\rangle}{\partial\tau}-\frac{\alpha_{p2}}{2}\left|A_{p2}\right\rangle+\frac{i8\gamma_{p2}}{9}P_{p2}\left|A_{p2}\right\rangle\\&+\left(\frac{i4\gamma_{p2}}{3}-\frac{1}{2}g_R^{p2,p1}\right)P_{p1}\left|A_{p2}\right\rangle+\left(\frac{i4\gamma_{p2}}{9}-\frac{1}{2}g_R^{p2,p1}\right)P_{p1}\hat{\mathbf{P}}_\mathbf{p1}\cdot\boldsymbol{\sigma}\left|A_{p2}\right\rangle\end{aligned} \tag{9}$$

#234455 - $15.00 USD Received 11 Feb 2015; revised 16 Apr 2015; accepted 19 Apr 2015; published 27 Apr 2015

$$\frac{\partial\left|A_{p1}\right\rangle}{\partial z}=-\delta\beta_1^{p1,s}\frac{\partial\left|A_{p1}\right\rangle}{\partial\tau}-\frac{\alpha_{p1}}{2}\left|A_{p1}\right\rangle-\frac{i}{2}\Omega^{p2,p1}\mathbf{b}\cdot\boldsymbol{\sigma}\left|A_{p1}\right\rangle+\frac{i8\gamma_{p1}}{9}P_{p1}\left|A_{p1}\right\rangle$$
$$+\left(\frac{i4\gamma_{p1}}{3}+\frac{1}{2}g_R^{p2,p1}\right)P_{p2}\left|A_{p1}\right\rangle+\left(\frac{i4\gamma_{p1}}{9}+\frac{1}{2}g_R^{p2,p1}\right)P_{p2}\hat{\mathbf{P}}_{\mathbf{p2}}\cdot\boldsymbol{\sigma}\left|A_{p1}\right\rangle \quad (10)$$

$$\frac{\partial\left|A_s\right\rangle}{\partial z}=-\frac{\alpha_s}{2}\left|A_s\right\rangle-\frac{i\beta_{2s}}{2}\frac{\partial^2\left|A_s\right\rangle}{\partial\tau^2}-\frac{i}{2}\Omega^{p2,s}\mathbf{b}\cdot\boldsymbol{\sigma}\left|A_s\right\rangle$$
$$+\left(\frac{i4\gamma_s}{3}+\frac{1}{2}g_R^{p2,s}\right)P_{p2}\left|A_s\right\rangle+\left(\frac{i4\gamma_s}{9}+\frac{1}{2}g_R^{p2,s}\right)P_{p2}\hat{\mathbf{P}}_{\mathbf{p2}}\cdot\boldsymbol{\sigma}\left|A_s\right\rangle \quad (11)$$
$$+\left(\frac{i4\gamma_s}{3}+\frac{1}{2}g_R^{p1,s}\right)P_{p1}\left|A_s\right\rangle+\left(\frac{i4\gamma_s}{9}+\frac{1}{2}g_R^{p1,s}\right)P_{p1}\hat{\mathbf{P}}_{\mathbf{p1}}\cdot\boldsymbol{\sigma}\left|A_s\right\rangle$$

where the subscript $p2$ and $p1$ denotes the 2nd order pump and 1st order pump respectively, and $\delta\beta_1^{i,j}=\beta_{1i}-\beta_{1j}$, $\Omega^{i,j}=\omega_i-\omega_j$ and $g_R^{i,j}$, with $i,j=p2,p1,s$. In deriving the equations, we have neglected XPM effect from signal to the 2nd order pump and 1st order pump, SPM effect of signal and assumed a non-depletion regime. The vector theory of 3rd order SRS can be obtained in the same manner, which are shown below:

$$\frac{\partial\left|A_{p3}\right\rangle}{\partial z}=-\delta\beta_1^{p3,s}\frac{\partial\left|A_{p3}\right\rangle}{\partial\tau}-\frac{\alpha_{p3}}{2}\left|A_{p3}\right\rangle+\frac{i8\gamma_{p3}}{9}P_{p3}\left|A_{p3}\right\rangle$$
$$+\left(\frac{i4\gamma_{p3}}{3}-\frac{1}{2}g_R^{p3,p2}\right)P_{p2}\left|A_{p3}\right\rangle+\left(\frac{i4\gamma_{p3}}{9}-\frac{1}{2}g_R^{p3,p2}\right)P_{p2}\hat{\mathbf{P}}_{\mathbf{p2}}\cdot\boldsymbol{\sigma}\left|A_{p3}\right\rangle \quad (12)$$
$$+\left(\frac{i4\gamma_{p3}}{3}-\frac{1}{2}g_R^{p3,p1}\right)P_{p1}\left|A_{p3}\right\rangle+\left(\frac{i4\gamma_{p3}}{9}-\frac{1}{2}g_R^{p3,p1}\right)P_{p1}\hat{\mathbf{P}}_{\mathbf{p1}}\cdot\boldsymbol{\sigma}\left|A_{p3}\right\rangle$$

$$\frac{\partial\left|A_{p2}\right\rangle}{\partial z}=-\delta\beta_1^{p2,s}\frac{\partial\left|A_{p2}\right\rangle}{\partial\tau}-\frac{\alpha_{p2}}{2}\left|A_{p2}\right\rangle-\frac{i}{2}\Omega^{p3,p2}\mathbf{b}\cdot\boldsymbol{\sigma}\left|A_{p2}\right\rangle+\frac{i8\gamma_{p2}}{9}P_{p2}\left|A_{p2}\right\rangle$$
$$+\left(\frac{i4\gamma_{p2}}{3}+\frac{1}{2}g_R^{p3,p2}\right)P_{p3}\left|A_{p2}\right\rangle+\left(\frac{i4\gamma_{p2}}{9}+\frac{1}{2}g_R^{p3,p2}\right)P_{p3}\hat{\mathbf{P}}_{\mathbf{p3}}\cdot\boldsymbol{\sigma}\left|A_{p2}\right\rangle \quad (13)$$
$$+\left(\frac{i4\gamma_{p2}}{3}-\frac{1}{2}g_R^{p2,p1}\right)P_{p1}\left|A_{p2}\right\rangle+\left(\frac{i4\gamma_{p2}}{9}-\frac{1}{2}g_R^{p2,p1}\right)P_{p1}\hat{\mathbf{P}}_{\mathbf{p1}}\cdot\boldsymbol{\sigma}\left|A_{p2}\right\rangle$$

$$\frac{\partial\left|A_{p1}\right\rangle}{\partial z}=-\delta\beta_1^{p1,s}\frac{\partial\left|A_{p1}\right\rangle}{\partial\tau}-\frac{\alpha_{p1}}{2}\left|A_{p1}\right\rangle-\frac{i}{2}\Omega^{p3,p1}\mathbf{b}\cdot\boldsymbol{\sigma}\left|A_{p1}\right\rangle+\frac{i8\gamma_{p1}}{9}P_{p1}\left|A_{p1}\right\rangle$$
$$+\left(\frac{i4\gamma_{p1}}{3}+\frac{1}{2}g_R^{p3,p1}\right)P_{p3}\left|A_{p1}\right\rangle+\left(\frac{i4\gamma_{p1}}{9}+\frac{1}{2}g_R^{p3,p1}\right)P_{p3}\hat{\mathbf{P}}_{\mathbf{p3}}\cdot\boldsymbol{\sigma}\left|A_{p1}\right\rangle \quad (14)$$
$$+\left(\frac{i4\gamma_{p1}}{3}+\frac{1}{2}g_R^{p2,p1}\right)P_{p2}\left|A_{p1}\right\rangle+\left(\frac{i4\gamma_{p1}}{9}+\frac{1}{2}g_R^{p2,p1}\right)P_{p2}\hat{\mathbf{P}}_{\mathbf{p2}}\cdot\boldsymbol{\sigma}\left|A_{p1}\right\rangle$$

#234455 - $15.00 USD Received 11 Feb 2015; revised 16 Apr 2015; accepted 19 Apr 2015; published 27 Apr 2015

$$\begin{aligned}\frac{\partial|A_s\rangle}{\partial z}=&-\frac{\alpha_s}{2}|A_s\rangle-\frac{i\beta_{2s}}{2}\frac{\partial^2|A_s\rangle}{\partial\tau^2}-\frac{i}{2}\Omega^{p3,s}\mathbf{b}\cdot\boldsymbol{\sigma}|A_s\rangle\\&+\left(\frac{i4\gamma_s}{3}+\frac{1}{2}g_R^{p3,s}\right)P_{p3}|A_s\rangle+\left(\frac{i4\gamma_s}{9}+\frac{1}{2}g_R^{p3,s}\right)P_{p3}\hat{\mathbf{P}}_{\mathbf{p3}}\cdot\boldsymbol{\sigma}|A_s\rangle\\&+\left(\frac{i4\gamma_s}{3}+\frac{1}{2}g_R^{p2,s}\right)P_{p2}|A_s\rangle+\left(\frac{i4\gamma_s}{9}+\frac{1}{2}g_R^{p2,s}\right)P_{p2}\hat{\mathbf{P}}_{\mathbf{p2}}\cdot\boldsymbol{\sigma}|A_s\rangle\\&+\left(\frac{i4\gamma_s}{3}+\frac{1}{2}g_R^{p1,s}\right)P_{p1}|A_s\rangle+\left(\frac{i4\gamma_s}{9}+\frac{1}{2}g_R^{p1,s}\right)P_{p1}\hat{\mathbf{P}}_{\mathbf{p1}}\cdot\boldsymbol{\sigma}|A_s\rangle\end{aligned}\tag{15}$$

where the subscript $p3$ denotes the 3rd order pump.

3. Noise mechanisms induced by pump RIN

It is well known that the intensity fluctuation of Raman pump laser source, which is characterized by RIN, will directly transfer to the signal's intensity through SRS effect. The mathematical model to evaluate such distortions was developed in [5] based on coupled power equations. The discussion was extended to 2nd order DRA case in [10], and the polarization dependence of such effect was further discussed in [11]. Since the mechanism of RIN transfer is clear and the mathematical modeling is complete, we will not discuss it in detail here.

Later on, it was pointed out in our previous work that pump RIN will deteriorate signal's phase through XPM effect [12]. The phase noise was defined as RPN. However, the discussion was confined in 1st order DRA. In the first part of this section, we will present a mathematical approach to calculate the statistical property of RPN in higher order DRA without dealing with the complex vector theory shown above. The proposed method is based on the numerical integration of coupled power equations. Moreover, we will discuss the pump RIN caused influence on signal's polarization in the second part.

3.1 RPN in higher order DRA

Note that both averaged XPM and XPolM will produce phase shift in principle. We here only deal with the phase noise induced by XPM. The phase noise caused by XPolM is generally polarization dependent and thus difficult to be calculated. Also its variance should be nine times smaller than that by XPM. We therefore can ignore its contribution.

The phase shift of signal caused by averaged XPM in 3rd order DRA is given by the integral:

$$\theta(L)=\frac{4\gamma_s}{3}\int_0^L\left(P_{p3}+P_{p2}+P_{p1}\right)\cdot dz\tag{16}$$

where L is length of the fiber link. If a small amount of modulation at angular frequency Ω is applied to the pumps, their power can be written as:

$$P_k(z,t)=\overline{P}_k(z)\cdot\left[1+m_k(z)\cdot\exp(i\cdot\Omega\cdot t)\right]\tag{17}$$

where $\overline{P}_k(z)$ is the average power, $m_k(z)$ is the complex modulation indices, with $k=p3,p2,p1$. The signal's phase fluctuation around the average phase shift is given by:

$$\Delta\theta(L,\Omega)=\frac{4\gamma_s}{3}\int_0^L\left[\overline{P}_{p3}(z)\cdot m_{p3}(z)+\overline{P}_{p2}(z)\cdot m_{p2}(z)+\overline{P}_{p1}(z)\cdot m_{p1}(z)\right]\cdot\exp(i\cdot\Omega\cdot t)\cdot dz\tag{18}$$

#234455 - $15.00 USD Received 11 Feb 2015; revised 16 Apr 2015; accepted 19 Apr 2015; published 27 Apr 2015

and the power spectral density (PSD) function of RPN:

$$PSD_{RPN}\left(L,\Omega\right)=\left|\Delta\theta\left(L,\Omega\right)\right|^2 \tag{19}$$

and the variance is:

$$\sigma_{RPN}^2=\int_{\nu_1}^{\nu_2}PSD_{RPN}\left(L,\Omega\right)\cdot d\Omega \tag{20}$$

where ν_1 and ν_2 are the lower and upper frequency of the receiver. Note that in order to obtain the PSD and the variance, only the power information of Raman pumps is needed. Using the expression $P=\langle A|A\rangle$, the Eqs. (12)–(14) can be simplified to the following coupled power equations if we neglect all polarization related terms:

$$\frac{\partial P_{p3}}{\partial z}=-\delta\beta_1^{p3,s}\frac{\partial P_{p3}}{\partial\tau}-\alpha_{p3}P_{p3}-g_R^{p3,p2}P_{p2}P_{p3}-g_R^{p3,p1}P_{p1}P_{p3} \tag{21}$$

$$\frac{\partial P_{p2}}{\partial z}=-\delta\beta_1^{p2,s}\frac{\partial P_{p2}}{\partial\tau}-\alpha_{p2}P_{p2}+g_R^{p3,p2}P_{p3}P_{p2}-g_R^{p2,p1}P_{p1}P_{p2} \tag{22}$$

$$\frac{\partial P_{p1}}{\partial z}=-\delta\beta_1^{p1,s}\frac{\partial P_{p1}}{\partial\tau}-\alpha_{p1}P_{p1}+g_R^{p3,p1}P_{p3}P_{p1}+g_R^{p2,p1}P_{p2}P_{p1} \tag{23}$$

Substitute Eq. (17) into Eqs. (21)–(23), we could yield a set of six coupled differential equations for the steady-state power and the complex spatial modulation indexes:

$$\frac{d\overline{P}_{p3}}{dz}=-\alpha_{p3}\overline{P}_{p3}-g_R^{p3,p2}\overline{P}_{p2}\overline{P}_{p3}-g_R^{p3,p1}\overline{P}_{p1}\overline{P}_{p3} \tag{24}$$

$$\frac{d\overline{P}_{p2}}{dz}=-\alpha_{p2}\overline{P}_{p2}+g_R^{p3,p2}\overline{P}_{p3}\overline{P}_{p2}-g_R^{p2,p1}\overline{P}_{p1}\overline{P}_{p2} \tag{25}$$

$$\frac{d\overline{P}_{p1}}{dz}=-\alpha_{p1}\overline{P}_{p1}+g_R^{p3,p1}\overline{P}_{p3}\overline{P}_{p1}+g_R^{p2,p1}\overline{P}_{p2}\overline{P}_{p1} \tag{26}$$

$$\frac{dm_{p3}}{dz}+i\cdot\Omega\cdot\delta\beta_1^{p3,s}\cdot m_{p3}=-g_R^{p3,p2}\overline{P}_{p2}m_{p2}-g_R^{p3,p1}\overline{P}_{p1}m_{p1} \tag{27}$$

$$\frac{dm_{p2}}{dz}+i\cdot\Omega\cdot\delta\beta_1^{p2,s}\cdot m_{p2}=g_R^{p3,p2}\overline{P}_{p3}m_{p3}-g_R^{p2,p1}\overline{P}_{p1}m_{p1} \tag{28}$$

$$\frac{dm_{p1}}{dz}+i\cdot\Omega\cdot\delta\beta_1^{p1,s}\cdot m_{p1}=g_R^{p3,p1}\overline{P}_{p3}m_{p3}+g_R^{p2,p1}\overline{P}_{p2}m_{p2} \tag{29}$$

Equations (24)–(29) can be solved by 4th order Runge-Kutta numerical integral method.

The mathematical treatment shown above can be used for any order DRA situation. Also it should be pointed out that such strategy can be generalized to take pump depletion into account. In depletion regime, Eqs. (21)–(23) should be modified by adding associated depletion terms. And an extra power equation describing signal is needed.

#234455 - $15.00 USD Received 11 Feb 2015; revised 16 Apr 2015; accepted 19 Apr 2015; published 27 Apr 2015

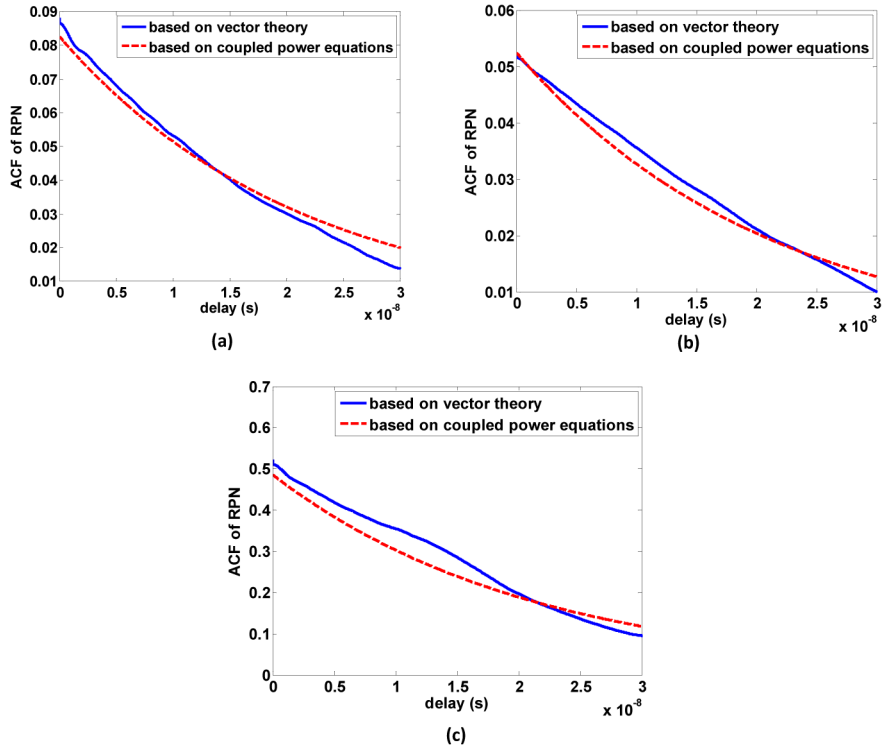

Fig. 1. ACF of RPN for (a) 1st order, (b) 2nd order, and (c) 3rd order DRA, where the RIN of 1st order pump in 1st order DRA, 2nd order pump in 2nd order DRA and 3rd order pump in 3rd order DRA is at −110 dB/Hz, and the RIN of the intermediate pumps in higher order DRA is at −140 dB/Hz.

The proposed approach can be operated much more easily than dealing with the vector theory based on coupled nonlinear Schrodinger equations, which is generally time-consuming. To test its validity, we compare the results obtained by the two methods. To solve the nonlinear Schrodinger equations, standard symmetric split-step Fourier method (SSFM) is used. Figure 1 illustrates the auto-correlation function (ACF) of RPN in 1st, 2nd and 3rd order DRA with PM-QPSK modulation format signal. The ACF is the Fourier transformation of PSD function. Statistical property of RPN can be obtained from its ACF. For example, the noise power, i.e., the variance, is the ACF at zero delay. In the simulations, the RIN of the primary pumps is at −110 dB/Hz, and the RIN of intermediate pumps is at −140 dB/Hz. More detailed descriptions of the simulation set-up can be found in the next section. According to Fig. 1, the calculations using the simplified approach agree well with the simulations based on vector theory, in both 1st and higher order DRA. It indicates that we can use this approach to predict the phase noise property in a simple manner.

3.2 RPolN

As is well known, XPolM effect will cause not only phase noise but also polarization crosstalk between two orthogonal polarized tributaries of a signal. During propagation through the fiber, the Stokes vector of signal will be precessed around the Stokes vector of pump at a rate determined by pump's power [6]. As long as both the pump's SOP and its power does not fluctuate at any time period, XPolM induced polarization crosstalk can be recovered by polarization demultiplexing algorithm embedded in DSP unit. However, neither of these conditions is satisfied in real case. The SOP of pump is altered by fiber birefringence in a random fashion, and meanwhile the pump has RIN. Therefore, the signal will suffer from

#234455 - $15.00 USD Received 11 Feb 2015; revised 16 Apr 2015; accepted 19 Apr 2015; published 27 Apr 2015

residual polarization crosstalk. We here name this type of noise the Relative Polarization Noise (RPolN) in order to keep the consistency with the previously defined terminologies (i.e., RIN and RPN). Since the interplay between random fiber birefringence and XPolM significantly complicates the process, we here will adopt numerical simulations to study the property of RPolN instead of looking for analytical treatment.

The residual polarization crosstalk can be evaluated by removing the transmitted x and y polarization tributary symbol from the carrier phase recovered signal. After the compensation of CD, PMD, laser frequency offset and carrier phase estimation, the output signal r are assumed as:

$$\begin{bmatrix} r_x \\ r_y \end{bmatrix} = \begin{bmatrix} \sqrt{1-w_{xy}^2} & w_{xy} \\ w_{yx} & \sqrt{1-w_{yx}^2} \end{bmatrix} \cdot \begin{bmatrix} s_x \\ s_y \end{bmatrix} \tag{30}$$

where s is the transmitted signal, w represents RPolN. If such polarization crosstalk is small, i.e., $w_{xy} \ll 1$ and $w_{yx} \ll 1$, they can be estimated as:

$$w_{xy} = \frac{r_x - s_x}{s_y}, \quad w_{yx} = \frac{r_y - s_y}{s_x} \tag{31}$$

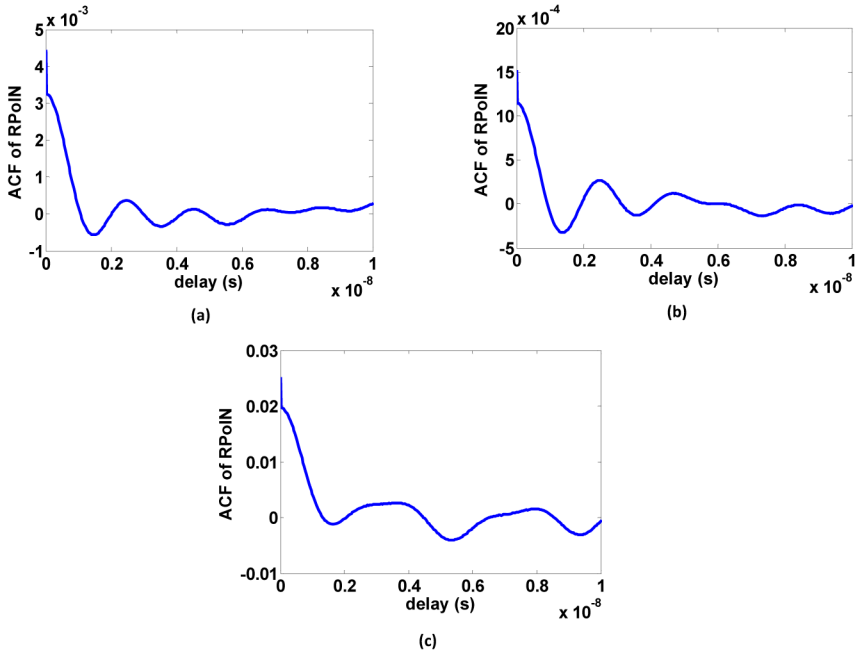

Fig. 2. ACF of RPolN for (a) 1st order, (b) 2nd order, and (c) 3rd order DRA, where the RIN of 1st order pump in 1st order DRA, 2nd order pump in 2nd order DRA and 3rd order pump in 3rd order DRA is at −110 dB/Hz, and the RIN of the intermediate pumps in higher order DRA is at −140 dB/Hz.

Figure 2 illustrates the ACF of RPolN in 1st, 2nd and 3rd order DRA. The simulation environment is the same as in Fig. 1. We can find that the ACF of RPolN has a half-magnitude width of less than 1 ns, which is over 15 times less than that of RIN and RPN. The cut-off frequency of RIN and RPN is typically several megahertz [5, 13], which depends on fiber parameters. The cut-off frequency of RPolN is dozens of megahertz. Hence, it cannot be tracked by traditional DSP polarization demultiplexing algorithm. The reason why RPolN is

#234455 - $15.00 USD Received 11 Feb 2015; revised 16 Apr 2015; accepted 19 Apr 2015; published 27 Apr 2015

faster can be understood as follows. The fiber random birefringence is usually rapidly varying (the fiber beat length is ~10 m). Therefore it can change the SOP of pump before the pump and signal walk off from each other. Such process will reduce the effectiveness of smooth-out effect offered by walk-off and thus increase the cut-off frequency of polarization crosstalk noise.

4. Pump RIN induced impairments in unrepeatered system

4.1 Simulation set-up

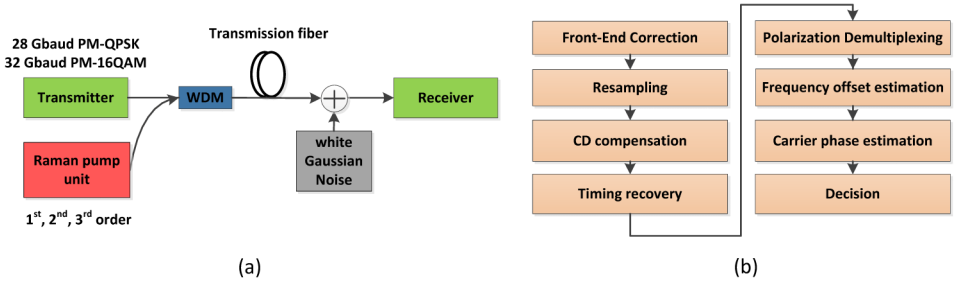

Fig. 3. (a) simulation set-up, and (b) DSP algorithm block diagram.

Table 1. Fiber parameters

Parameter	Value	Parameter	Value
Fiber length	150 km	A_{eff} at 193.1 THz	140 μm^2
attenuation at 193.1 THz	0.178 dB/km	dispersion at 193.1 THz	17 ps/nm/km
attenuation at 206.25 THz	0.223 dB/km	Dispersion slope	0.08 ps/nm^2/km
attenuation at 219.4 THz	0.352 dB/km	PMD parameter	0.1 ps/sqrt(km)
attenuation at 232.55 THz	0.450 dB/km	Correlation length	100 m

Figure 3(a) illustrates the MATLAB simulation set-up. The transmitter generates multi-level modulation format signal with zero linewidth. Two types of modulation formats with 32768 symbols are simulated: 28 Gbaud PM-QPSK and 32 Gbaud PM-16QAM. Single channel is used here to avoid XPM effect between signals. The input power is limited to −20 dBm to minimize SPM effect. Forward Raman pumps, which are polarization multiplexed to minimize the polarization dependent gain, amplify the signal as they propagate along the transmission fiber. The fiber parameters are given in the Table 1. Although in practical unrepeatered systems, usually more than one section of fiber span and more than one amplifier are used, we simplify the system to only one section of fiber containing only forward pumped DRA. This is because what we try to focus is the forward Raman pump RIN induced impairments. The power of pump decays hugely after hundreds of kilometers propagation, and thereby causing negligible influence on the signal for the rest of the span. In this paper, we use 150-km-long fiber to do the simulation, which is long enough for the interaction between pump and signal, and can save simulation time. Also as shown in the unrepeatered transmission experiment using forward pumped DRA [16], the fiber length from the transmitter side to the first remote optically pumped amplifier (ROPA) is 133.7 km, which again demonstrates this point. The propagation of lights inside the fiber is governed by the vector theory based on coupled nonlinear Schrodinger equations. Standard symmetric SSFM with adaptive step size is used to solve the equations and yield converged results. The additive white Gaussian noise (AWGN) is added at the output of the fiber to determine the desired signal-to-noise ratio (SNR) level at given bit error ratio (BER). We assume an ideal coherent receiver, i.e., the local oscillator (LO) has zero linewidth and zero frequency offset with respect to the signal. Therefore, the only noisy source in our simulation is the Raman pump's intensity fluctuation. The pump RIN is modeled by a flat electrical noise spectrum. Although this is unrealistic as RIN follows the intrinsic frequency response of the laser with peaks due

#234455 - $15.00 USD Received 11 Feb 2015; revised 16 Apr 2015; accepted 19 Apr 2015; published 27 Apr 2015

to the electron-photon resonance (caused by the interaction of the electron and photon populations), it can represent worst case RIN. The noise bandwidth is set to be 1 GHz.

Figure 3(b) illustrates the block diagram of DSP algorithms. Since we assumed an ideal receiver, front-end correction and frequency offset estimation are skipped. Frequency domain equalization is used to compensate CD. The Gardner algorithm is used to do timing recovery. Single stage CMA algorithm with 13 taps is used to demultiplex polarizations of PM-QPSK signal, and dual stages consisting of CMA and RD-CMA with both 13 taps are used to demultiplex PM-16QAM signal. At carrier phase estimation (CPE) section, sliding window Viterbi-and-Viterbi algorithm with 31 blocksize and QPSK partitioning algorithm with 101 blocksize are used to recover the carrier phase of PM-QPSK and PM-16QAM signal respectively.

4.2 Transmission Penalties for PM-QPSK systems

Most of today's unrepeatered transmission experiments have used PM-QPSK modulation format to deliver 100 G interface speed [16, 17, 22]. We first analyze the pump RIN induced impairments in this situation.

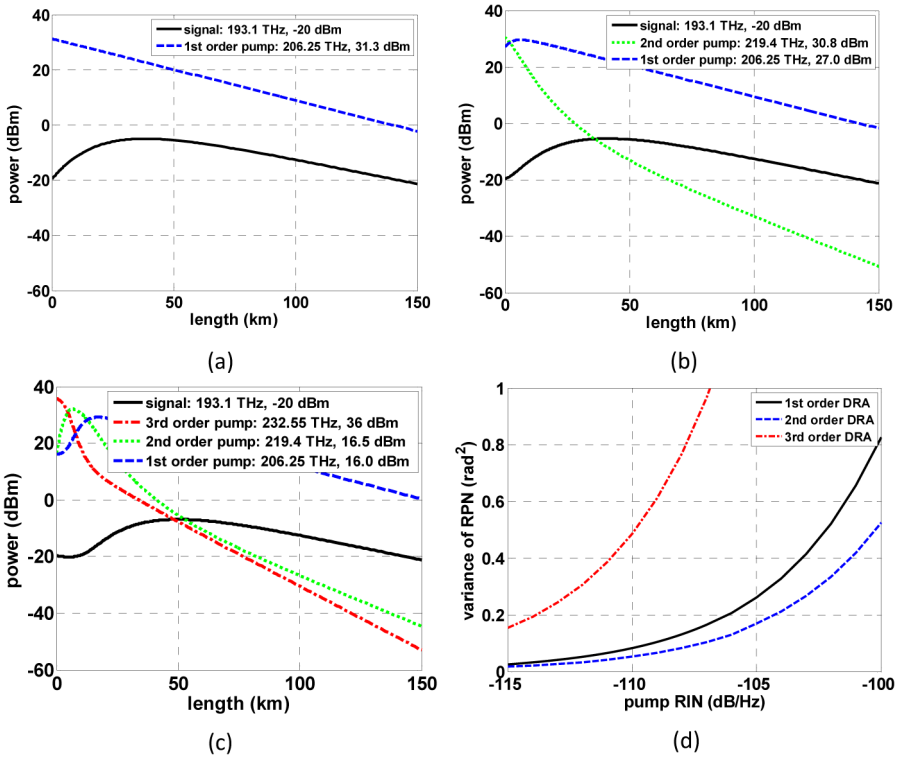

Fig. 4. Power evolution for (a) 1st order DRA, (b) 2nd order DRA and (c) 3rd order DRA, (d) the calculated variance of RPN in 1st, 2nd and 3rd order DRA.

The power evolution is shown in Fig. 4 (a)–(c) for 1st, 2nd and 3rd order DRA where the on-off gain of signal is all 25.5 dB. The frequency shift between adjacent light is 13.15 THz, where is the peak of Raman gain efficiency. The input power of each light is also shown. Note that in all cases, the power of light has been decreased to below 0 dBm after 150-km propagation. The interaction between lights can be ignored at further region. The calculated variance of RPN for three cases is shown in Fig. 4(d). We can find that the variance is the largest in 3rd order DRA because the input power is the highest. Although the input power of 2nd order DRA (1700 mW in total) is higher than that of 1st order (1350 mW in total), the

#234455 - $15.00 USD Received 11 Feb 2015; revised 16 Apr 2015; accepted 19 Apr 2015; published 27 Apr 2015

variance is slightly smaller. This can be explained by the walk-off effect. The walk-off between two lights is associated with their group velocities $V = c/n$, where c is the speed of light in vacuum, and n is the group refractive index of fiber core and can be computed by the Sellmeier function [10], i.e., $n = n_0 + (S_0/8)\cdot\left(\lambda - \lambda_0^2/\lambda^2\right)\cdot c$, where n_0 and S_0 are the group refractive index (1.47 in our simulation) and the dispersion slope at the zero dispersion wavelength λ_0, respectively. The computed walk-off between 1st, 2nd, 3rd order pump and the signal is 1.0922, 1.5406 and 1.4592 ps/m, respectively. Therefore, the walk-off between 1st order pump and signal is less than that between 2nd order pump and signal. The noise transfer process is then more efficient. Although we have only shown the variance of phase noise, we can expect the similar trend of penalty curve.

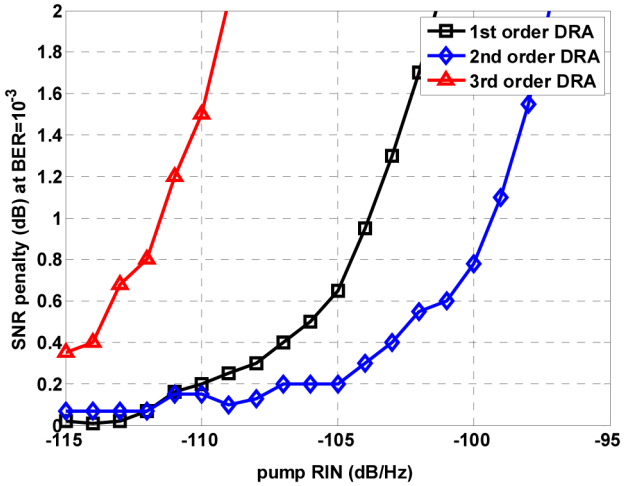

Fig. 5. The SNR penalty for PM-QPSK at BER = 10^{-3} for 1st, 2nd, and 3rd order DRA.

The SNR penalty is evaluated for three different order DRA and is shown in Fig. 5. The target BER is 10^{-3}. In the simulations, the RIN of intermediate pumps is fixed at −140 dB/Hz, which is a typical RIN level for laser diode. Similar curve compared to Fig. 4(d) can be found, where 3rd order DRA has the largest penalty and 1st order DRA has larger penalty compared to 2nd order case. It is a reasonable result since 3rd order DRA has the highest variance of noise while 2nd order DRA has the lowest one. The required RIN at 1 dB SNR penalty is around −106, −99.5 and −111.5 dB/Hz for 1st, 2nd and 3rd order DRA.

Since in real systems, semiconductor laser diode (LD) is usually served as pumping source for 1st order amplifier, whose RIN can be as low as −140 dB/Hz. Almost no penalty can be observed at such RIN level. Even if one uses fiber laser as the pump, whose typical RIN is −105 dB/Hz, the penalty is around 0.6 dB and can be tolerated. For 2nd order DRA, the required RIN is also higher than −105 dB/Hz. These two findings suggest that the penalty induced by 1st and 2nd order Raman pump RIN can be ignored for PM-QPSK based unrepeatered system. Recent experimental studies presented in [16, 17, 22] using 1st and 2nd order Raman amplifier have all successfully achieved error-free PM-QPSK unrepeatered transmissions. However, upgrading the amplifier to 3rd order may introduce non-negligible penalty. Pump RIN suppression technique is needed to avoid such penalty.

4.3 Transmission Penalties for PM-16QAM systems

To further increase the capacity of unrepeatered system, higher-order modulation format is necessary. PM-16QAM is suggested to be a good candidate for the next generation system. There are a few experimental studies using PM-16QAM [23, 24]. It will be interesting to

#234455 - $15.00 USD Received 11 Feb 2015; revised 16 Apr 2015; accepted 19 Apr 2015; published 27 Apr 2015

study pump RIN induced impairments on PM-16QAM based unrepeatered system. The system set-up and parameters are the same as those used in PM-QPSK. The result is shown in Fig. 6.

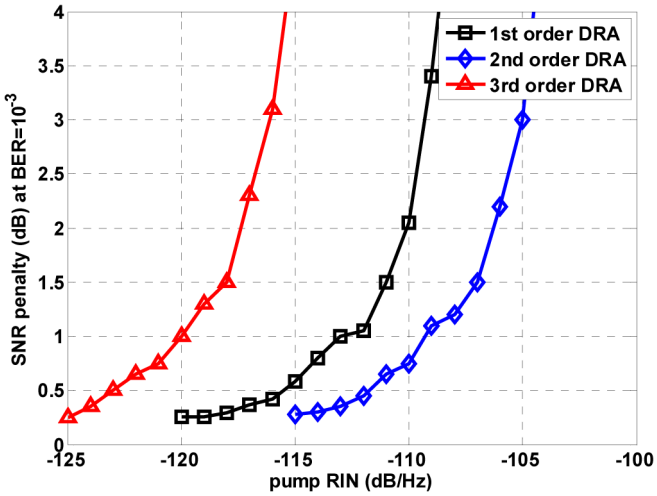

Fig. 6. SNR penalties for PM-16QAM at BER = 10^{-3} for 1st, 2nd, and 3rd order DRA.

It can be found from the figure that PM-16QAM suffers larger penalty compared to PM-QPSK. The required pump RIN at 1 dB SNR penalty is around −112, −109 and −120 dB/Hz for 1st, 2nd and 3rd order DRA respectively. The results indicate that for PM-16QAM based unrepeatered systems, LD can be used as 1st order pumping source with negligible degradation, however, fiber lasers with a typical −105 dB/Hz RIN cannot satisfy performance requirement. Either pump RIN suppression or reducing on-off gain provided by forward pumps is indispensable.

5. Discussions

RIN, RPN and RPolN are the noises imprinted on three different dimensions. RIN causes amplitude fluctuation, RPN causes phase fluctuation, while RPolN affects both dimensions by means of crosstalk. To provide an intuitive picture how these effects distort the signal, we can solve the coupled equations by separating the nonlinear effects.

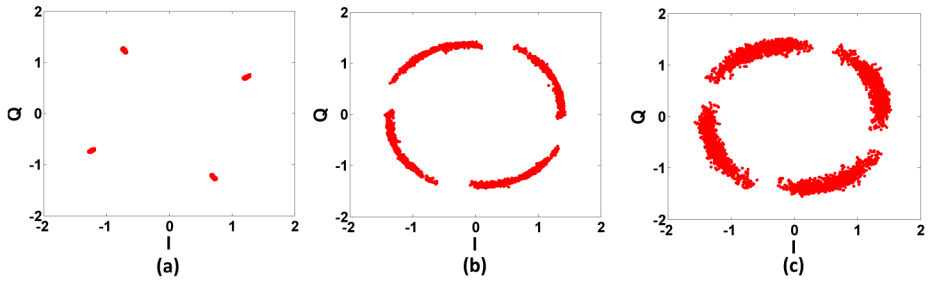

Fig. 7. The constellation diagram of x-polarization QPSK signal with (a) RIN only, (b) RIN and RPN, (c) RIN, RPN and RPolN. The 2nd order forward pump with −105 dB/Hz is used.

Figure 7 plots the constellation diagrams (before CPE stage) of x-polarization QPSK signal at different conditions. XPM and XPolM effects were turned off at first to give an image of RIN distortions and the result is shown in Fig. 7(a). Fluctuation at radial direction can be seen due to RIN. Next, only XPolM was turned off. The resulting constellation is

#234455 - $15.00 USD Received 11 Feb 2015; revised 16 Apr 2015; accepted 19 Apr 2015; published 27 Apr 2015

shown in Fig. 7(b), where the signal is distorted by both RIN and RPN. Deviation on the angular distribution clearly shows the impact of RPN. At the final step, all the effects were taken into consideration. The constellation is shown in Fig. 7(c). Compared to Fig. 7(b), each trace was thicker as a result of crosstalk induced by RPolN.

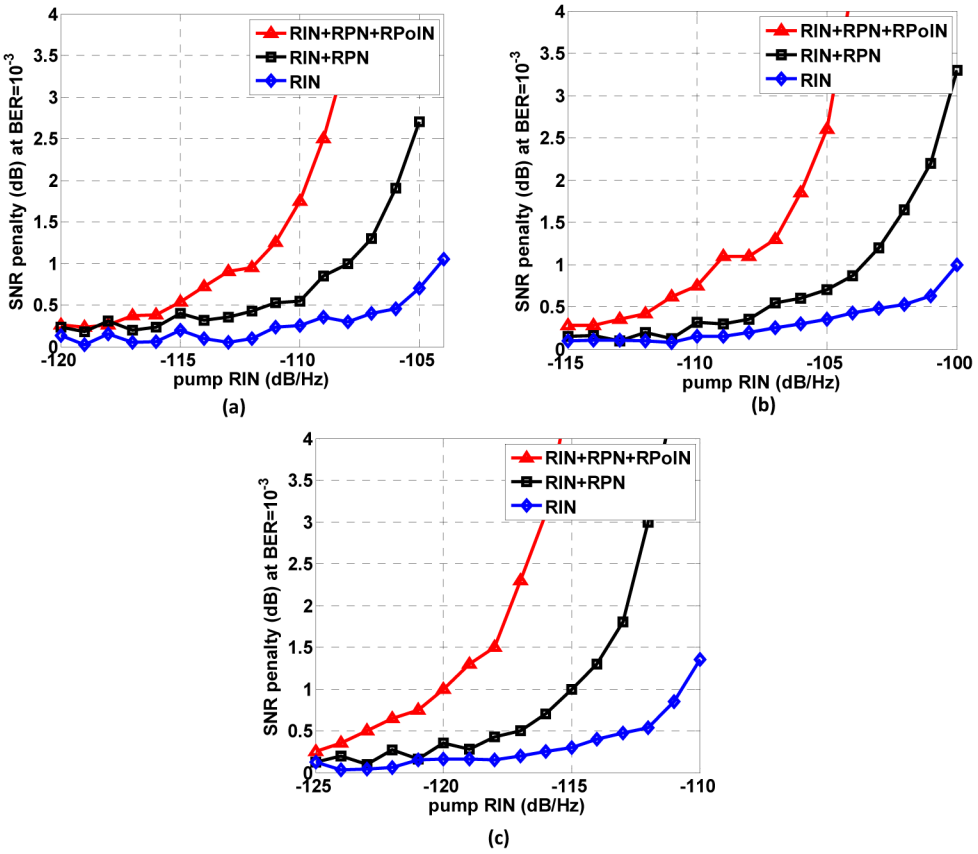

Fig. 8. SNR penalty for PM-16QAM in (a) 1st order, (b) 2nd order, and (c) 3rd order DRA.

We can also illustrate the corresponding SNR penalty curve at these conditions. The result is shown in Fig. 8 for PM-16QAM. It can be found that RPN and RPolN will cause about the same extra penalty in 1st, 2nd and 3rd order DRA. The simulation of QPSK signal can also be done. However, cycle slips would occur at high RPN region. Detection and correction of cycle slip is beyond the scope of this paper, and thus we will not discuss it further.

Another interesting aspect to discuss is the performance of DSP algorithms in mitigating these impairments. We have discussed in [13] the mitigation of RPN using modified CPE algorithm. It can be achieved by optimization of averaging weights according to minimum mean-square error (MMSE) criterion. And it was proposed in [26] an efficient polarization crosstalk mitigation algorithm called nonlinear polarization crosstalk canceller (NPCC).

#234455 - $15.00 USD Received 11 Feb 2015; revised 16 Apr 2015; accepted 19 Apr 2015; published 27 Apr 2015

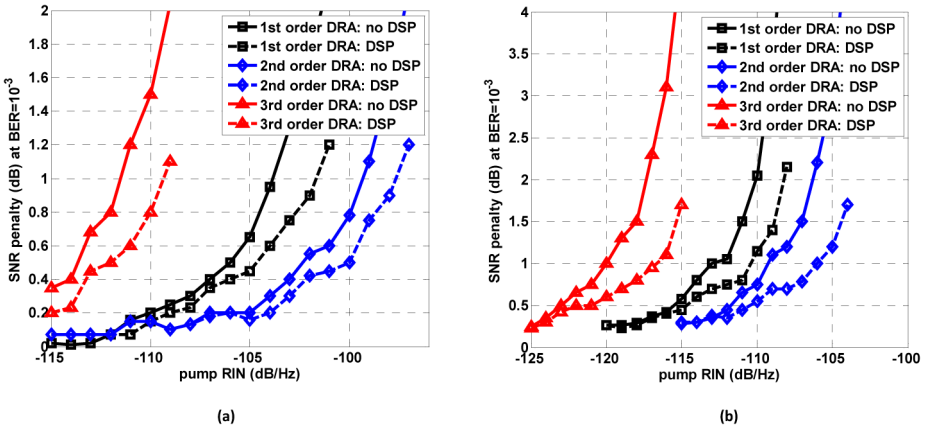

Fig. 9. The SNR penalty with and without using mitigation algorithms for (a) PM-QPSK and (b) PM-16QAM.

Figure 9 shows the simulation results for PM-QPSK and PM-16QAM systems. The NPCC with optimal filter length is inserted after CPE. Details of both mitigation algorithms can be found in [13] and [26]. According to Fig. 9, the DSP algorithms can indeed reduce the SNR penalty, thereby increasing the required pump RIN level. However, the improvement is limited. RIN tolerance has less than 3 dB increase for both modulation formats.

6. Conclusions

In this paper, we presented the vector theory of 1st and higher order DRA utilizing Jones-matrix formalism. It was shown that in addition to RIN and RPN, pump RIN will also induce polarization crosstalk to multi-level modulation format signals through XPolM effect. Simplified mathematical approach without dealing with complex vector theory was obtained to predict the stochastic property of RPN generated in higher order DRA. Simulations suggested that PM-QPSK can tolerate up to −106, −99.5 and −111.5 dB/Hz pump RIN in 1st, 2nd and 3rd order forward pumped unrepeatered systems, while the corresponding RIN tolerance for PM-16QAM is −112, −109 and −120 dB/Hz, respectively. Further studies showed that RPN and RPolN have about the same impact on performance. And if using an optimized CPE and NPCC algorithms, the RIN tolerance can be increased by less than 3 dB. The model presented in this paper is helpful for the design of multi-level modulation format signal based unrepeatered transmission systems using DRA. The conclusions made in here can be served as a guideline on the selection and screening of Raman pumping source in future's unrepeatered transmission experiments. Further investigation of more powerful algorithms for impairment mitigation in DRA systems will be conducted in future.

Acknowledgments

This work was supported by the Hong Kong Polytechnic University Project H-ZDA9, the 863 High Technology Plan of China (2013AA013402), the National Natural Science Foundation of China (NSFC) under Grant No. 61331010, the Fundamental Research Funds for the Central Universities', HUST: 2013TS052, and the Program for New Century Excellent Talents in University (NCET-13-0235).